Vibrational modes of adsorbed atoms

W. R. Lawrence* and R. E. Allen

Department of Physics, Texas A&M University, College Station, Texas 77843
(Received 1 June 1976)

The vibrational spectra have been calculated for seven model adsorbate-substrate systems.

I. INTRODUCTION

Recently,[1] we reported calculations of heat capa-
cities of adsorption for seven model adsorbate-
substrate systems—^{4}He on Xe, Ne on Ar, Kr, and
Xe, Ar on Kr and Xe, and Kr on Xe, with the sub-
strate having a (100) face and the adsorbed atoms
going down in registry with the substrate. We
thought that there might be some interest in a de-
tailed description of the vibrational spectra of
these systems, since previous treatments of the
vibrational modes of adsorbates have involved
mass-defect models,[2] so we have given such a
description in the present paper. The method of
calculation and details of the model are the same
as in Ref. 1; in particular, the expansion at the
surface due to zero-point vibrations (important
for ^{4}He and Ne adsorbates) is included.

II. PHONON-DISPERSION CURVES

In Figs. 1–7, the dimensionless frequency ω^*
is plotted as a function of the two-dimensional
wave vector $\bar{q}$ along the symmetry lines[3] $\bar{\Gamma}\bar{X}$, $\bar{X}\bar{M}$,
and $\bar{M}\bar{\Gamma}$; ω^* is related to the frequency ω by ω^*
$\equiv (m_s\sigma_s^2/\epsilon_s)^{1/2}\omega$, where m_s, σ_s, and ϵ_s are the
atomic-mass and Lennard-Jones–potential param-
eters for the substrate. These results are for 11
layer slabs with nine layers of substrate sand-
wiched between two adsorbate layers. We have
labeled each surface mode by a number which
indicates the plane in which its amplitude is larg-
est (with the plane of adsorbed atoms represented
by 1, the first plane of substrate atoms labeled
by 2, etc.) and by letters which indicate the domi-
nant polarization (with L representing longitudinal
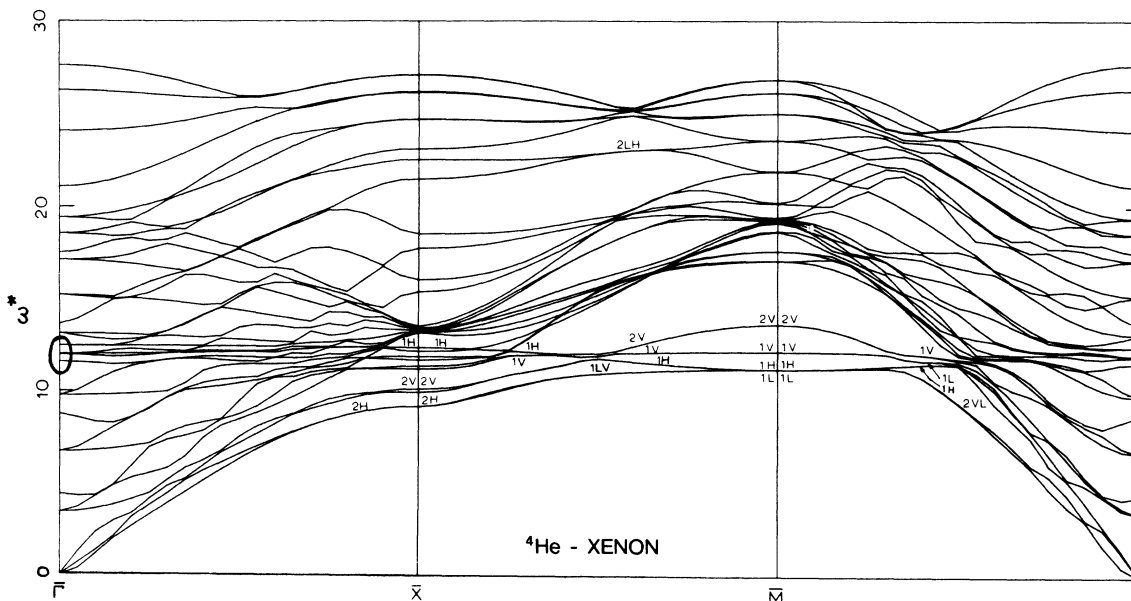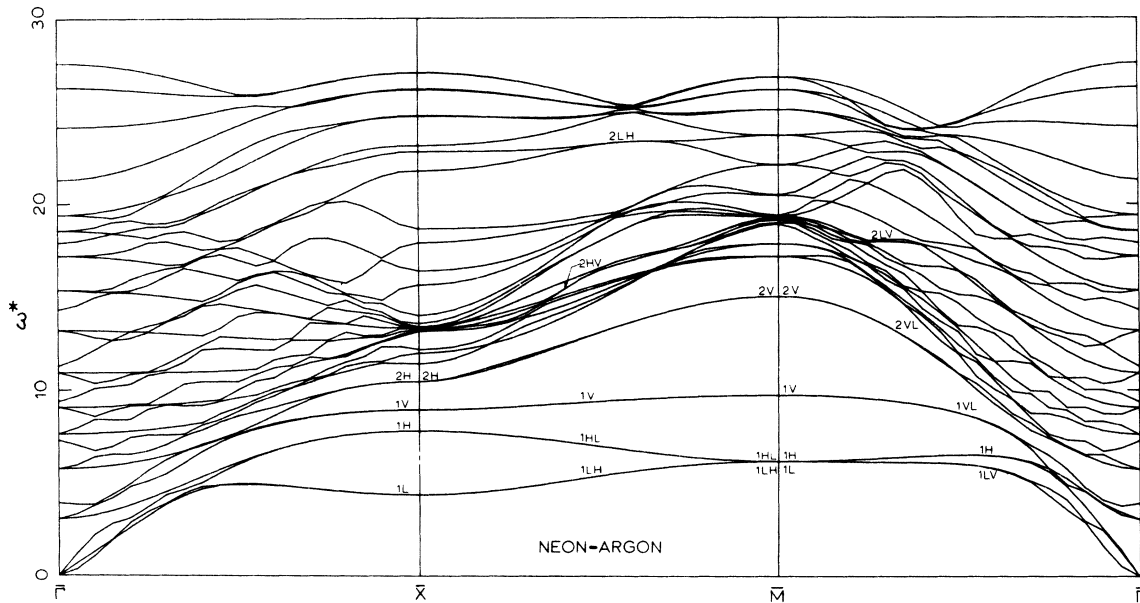polarization, H representing "horizontal" polari-

FIG. 1. Dimensionless frequency ω^* vs two-dimensional wave vector $\bar{q}$, along symmetry lines, for ^{4}He on Xe. There
are nine substrate layers between two adsorbate layers, and thus $3 \times (9+2) = 33$ modes per $\bar{q}$.

FIG. 2. ω^* vs $\bar{q}$ for Ne on Ar.

zation, parallel to the surface and transverse to the direction of propagation, and V representing "vertical" polarization, transverse and perpendicular to the surface). For example, in Fig. 1, the

mode labeled $2LH$ along $\overline{XM}$ has its maximum in the outermost layer of substrate atoms and is mostly longitudinal, with less transverse "horizontal" polarization and still less "vertical" polar-
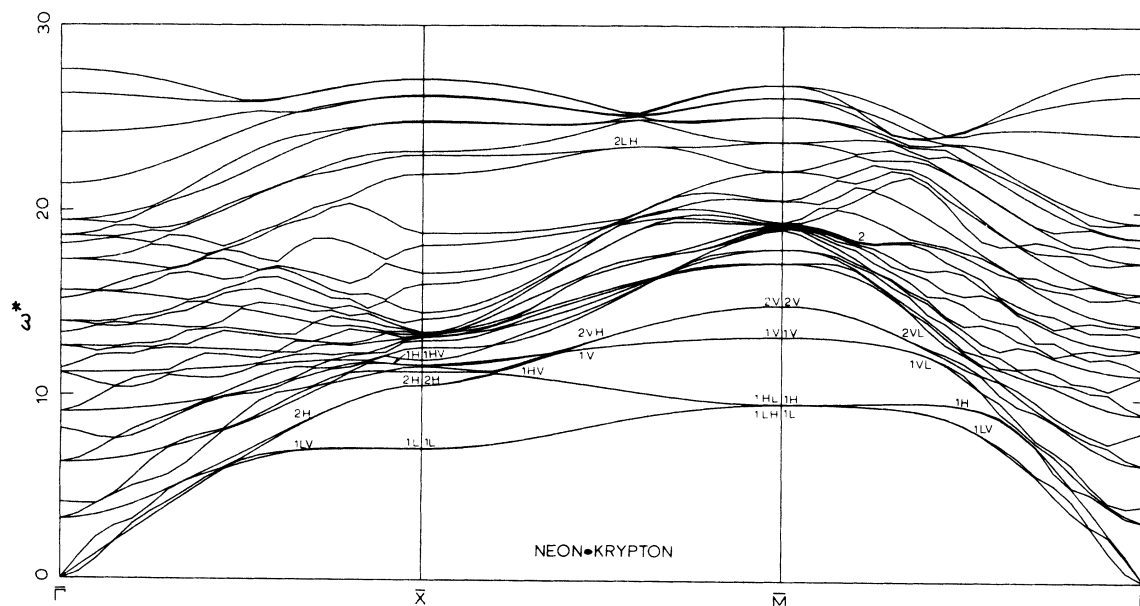
FIG. 3. ω^* vs $\bar{q}$ for Ne on Kr.
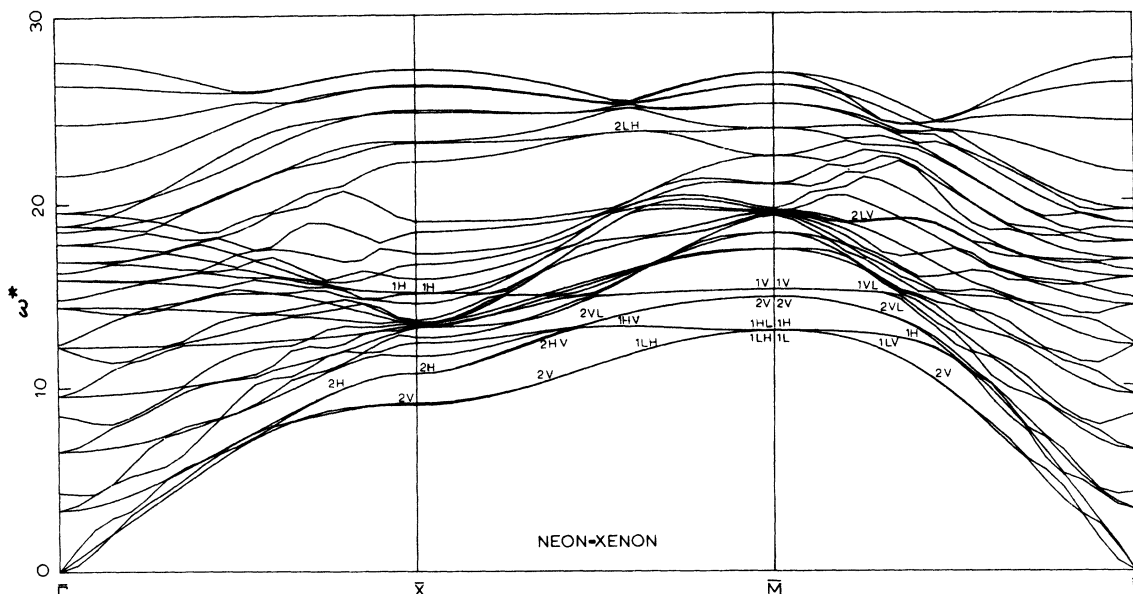
FIG. 4. $\omega*$ vs $\bar{q}$ for Ne on Xe.

ization. The amplitude and polarization of each mode in a given plane were determined by inspecting the associated eigenvector $\vec{\xi}(m)$.[3]

III. DISCUSSION OF RESULTS

A. ^{4}He on Xe

Because the He-Xe interaction is weak compared to the Xe-Xe interaction, the surface modes for the clean Xe surface are largely unaffected by the He overlayer in Fig. 1. In particular, the mode labeled $2H$ along $\bar{\Gamma}\bar{X}$, $2V$ near $\bar{M}$, and $2VL$ on the right-hand side of $\bar{M}\bar{\Gamma}$ corresponds to S_1 of Allen et al.[3] (see Fig. 10) for the clean Xe surface; and the mode labeled $2V$ near $\bar{X}$ corresponds to S_4. There is, of course, hybridization of these modes with the new ones introduced by the He overlayer, between $\bar{X}$ and $\bar{M}$ and between $\bar{M}$ and $\bar{\Gamma}$. The mode
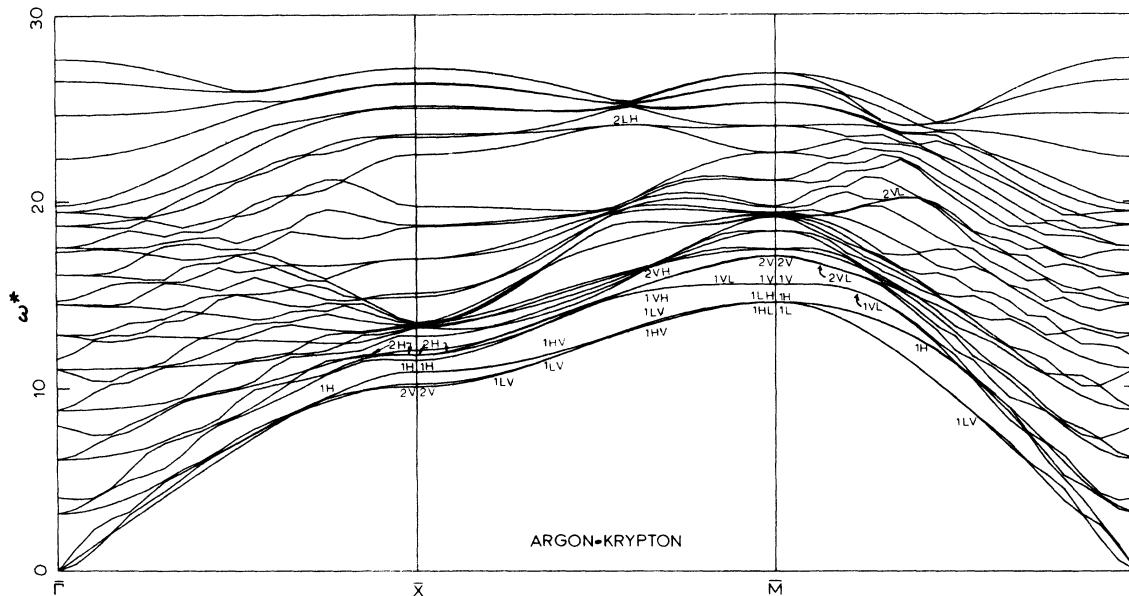
FIG. 5. $\omega*$ vs $\bar{q}$ for Ar on Kr.
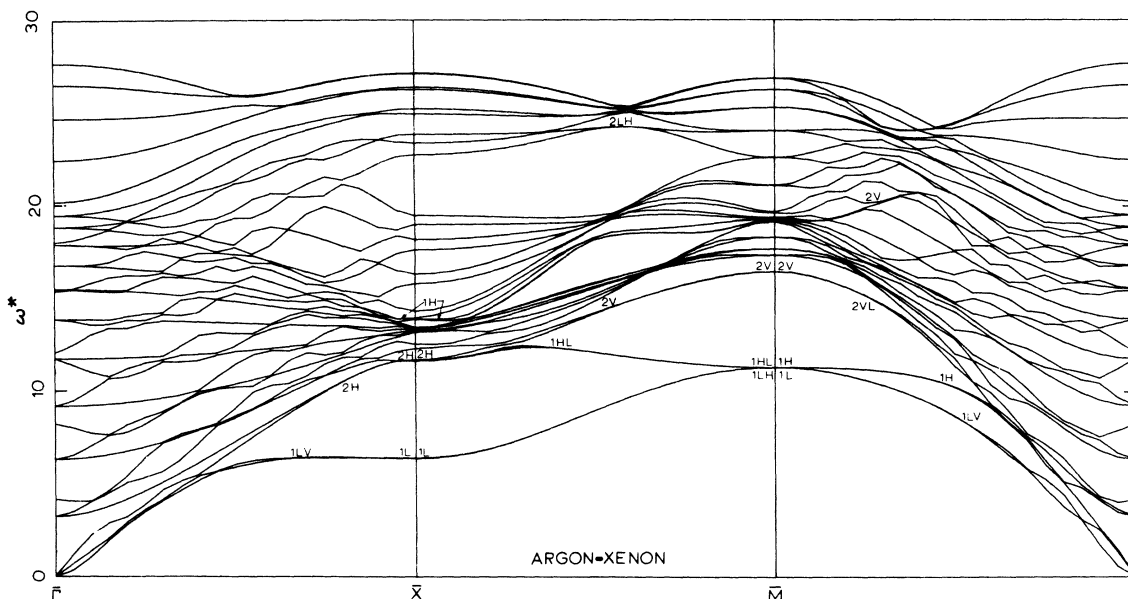
FIG. 6. ω^* vs $\bar{q}$ for Ar on Xe.

labeled $2LH$ along $\overline{XM}$ corresponds to S_6 of Ref. 3 for the clean Xe surface.

In Fig. 8, a graph of the amplitude $|\vec{\xi}(m)|^2$ is shown for $1H$ at $\overline{X}$. It is interesting that the modes associated with the He overlayer persist to $\overline{\Gamma}$ as resonances at $\omega^* \simeq 12$, surrounded by an oval curve in Fig. 1. Graphs of $|\vec{\xi}(m)|^2$ for these resonances are also given in Fig. 8.

B. Ne on Ar

The lowest surface mode branches in Fig. 2 are very clear examples of the "principal" surface modes[2] associated with an adsorbate; there are three modes associated with the three directions of vibration (L, H, V) for the adsorbate atoms. In addition, the branch labeled $2H$ at $\overline{X}$ at $2V$ at $\overline{M}$
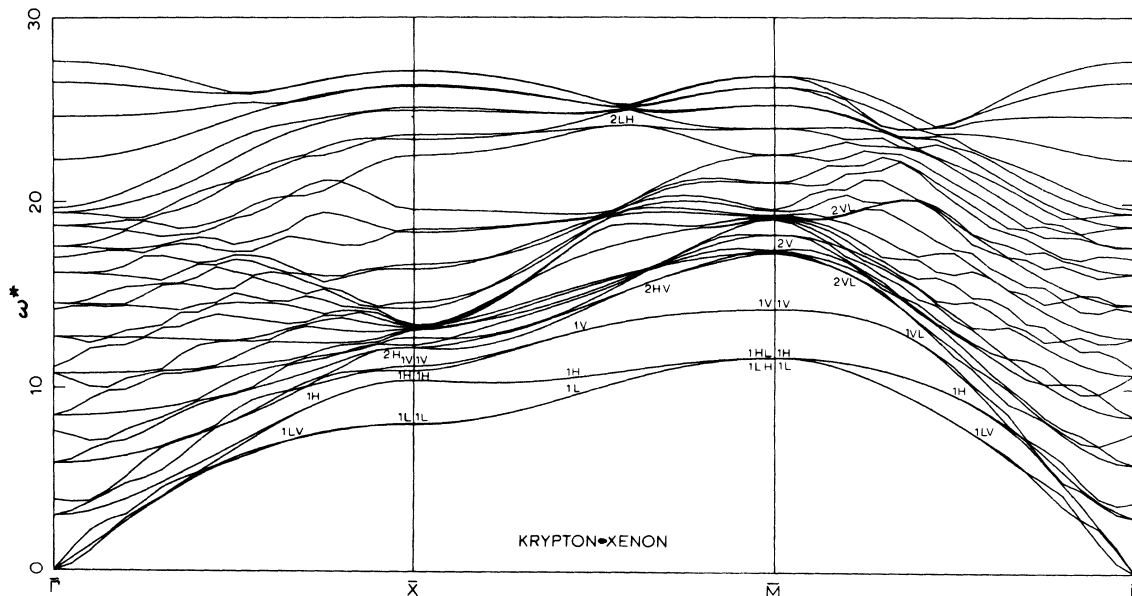
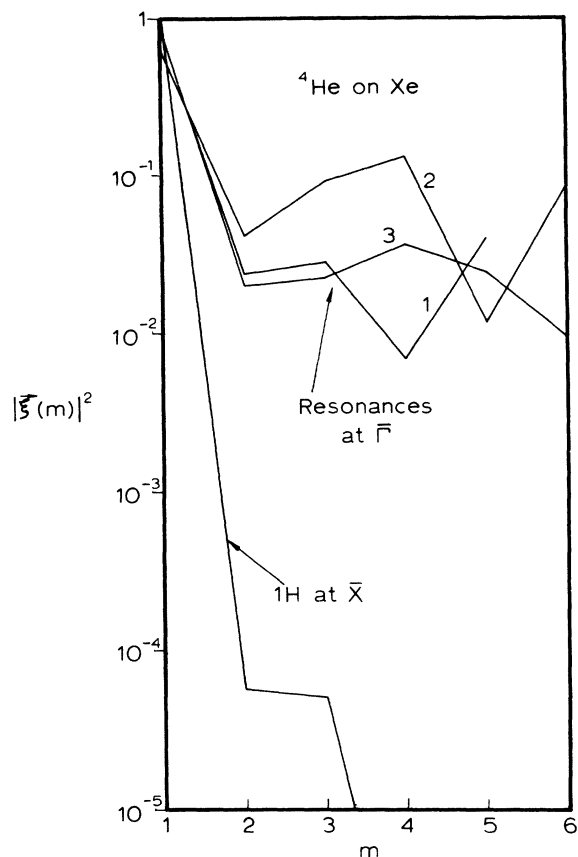FIG. 7. ω^* vs $\bar{q}$ for Kr on Xe.

FIG. 8. $|\vec{\xi}(m)|^2$ vs m for surface mode $1H$ at $\bar{X}$ in Fig. 1, and for the resonances at $\bar{\Gamma}$ enclosed by an oval curve. Here $m = 1$ for the layer of adsorbate atoms, $m = 2$ for the first layer of substrate atoms, etc. "1" labels the highest pair of resonance modes, having in-plane polarization; "2" labels a pair just below, also with in-plane polarization; and "3" labels the last (non-degenerate) pair with polarization perpendicular to the surface. These resonances are principally associated with vibrations of the adsorbed ^{4}He atoms.

clearly corresponds to S_1 of Ref. 3, Fig. 10.

Figure 2 can be compared with Fig. 3 of Ref. 2, where the ordering of $1V$ and the degenerate pair $1L$, $1H$ at $\bar{M}$ is inverted. This comparison shows an interesting failure of the mass-defect model: In this model, the restoring force for in-plane vibrations of adsorbate atoms is larger than the restoring force for vibrations perpendicular to the surface, so the $1L$ and $1H$ modes lie above the $1V$ mode. In the present model, the restoring force for in-plane vibrations is smaller, because the Ne-Ne interaction is weak compared to the Ne-Ar interaction, and the $1L$ and $1H$ modes lie below the $1V$ mode.

In comparisons with the mass-defect model, incidentally, one should regard the "mass" of a particle as really being a measure of the mass divided

by an effective force constant; i.e., if M_a and M_s are the masses of adsorbate and substrate atoms in the mass-defect model, then we should take

$$\frac{M_a}{M_s} = \frac{m_a/k_a}{m_s/k_s} \, ,$$

where m_a and m_s are the real adsorbate and substrate atomic masses, and k_a and k_s are characteristic force constants for adsorbate and substrate. It is evident that in Fig. 2 the adsorbate is "heavier" than the substrate $(M_a > M_s)$ in this interpretation, because the weakness of the adsorbate interactions $(k_a < k_s)$ more than compensates for the lightness of the adsorbate atoms $(m_a < m_s)$.

C. Ne on Kr

The three "principal" surface modes for the adsorbate are visible near $\bar{M}$ in Fig. 3, although the frequencies of the principal modes are higher for Ne on Kr (relative to the bulk Kr spectrum) than they are for Ne on Ar (relative to the bulk Ar spectrum). The substrate mode S_1 is again evident, as $2H$ near $\bar{X}$ and $2V$ near $\bar{M}$, although it hybridizes twice with the adsorbate modes, $1HV$ and $1V$, along $\bar{X}\bar{M}$. The mode labeled "2" is a second-layer mode with sagittal-plane polarization.

D. Ne on Xe

The relative frequencies of the "principal" surface modes in Fig. 3 have again been raised, but the qualitative features are about the same as for Ne on Kr. The mode labeled $2V$ at $\bar{X}$ is almost as large in the first (adsorbate) layer as in the second (substrate) layer. The $1H$ mode at $\bar{X}$ is a pure surface mode. Just to the right of $\bar{X}$ in Fig. 4, this mode becomes a resonance, until it emerges from the bulk bands between $\bar{X}$ and $\bar{M}$. Plots of $|\vec{\xi}|^2$ for this mode are given in Fig. 9 for 11 evenly spaced points along $\bar{X}\bar{M}$, with point 1 being $\bar{X}$, point 2 just to the right of $\bar{X}$, etc., and point 11 being $\bar{M}$.

E. Ar on Kr

The clean Kr surface mode S_1 is visible in Fig. 5 as $2H$ at $\bar{X}$ and $2V$ at $\bar{M}$. The three principal adsorbate modes exist at $\bar{M}$, as usual, and the lowest of these remain remarkably close together at $\bar{X}$ as $1H$ and $2V$. As in the discussion of Ne on Xe, just above, $2V$ has a large amplitude in the adsorbate even though $|\vec{\xi}|^2$ reaches a maximum in the first substrate layer. This can be seen in Fig. 10, where we have graphed $|\vec{\xi}|^2$ for the surface modes at $\bar{X}$ and $\bar{M}$. Graphs of the corresponding modes in Figs. 1–4, 6, and 7 show similar behavior.
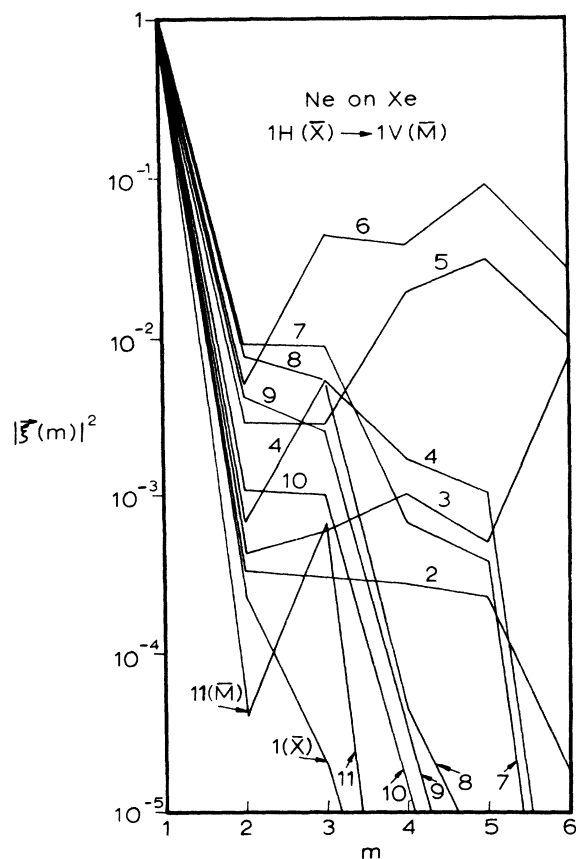
FIG. 9. $|\vec{\xi}(m)|^2$ vs m for $1H$ at $\bar{X}$ (point 1), $1V$ at $\bar{M}$ (point 11), and a series of resonances and surface modes between these points along $\bar{X}\bar{M}$ in Fig. 4.

FIG. 10. $|\vec{\xi}(m)|^2$ vs m for surface modes at $\bar{X}$ and $\bar{M}$ in Fig. 5.

F. Ar on Xe

There are no features in Fig. 6 that have not been discussed above.

G. Kr on Xe

All three principal adsorbate modes persist from $\bar{M}$ to $\bar{X}$. In this case, as for Ar on Kr and Ar on Xe, the adsorbate-substrate interactions are strong enough to raise the substrate surface mode frequencies considerably.

IV. CONCLUSION

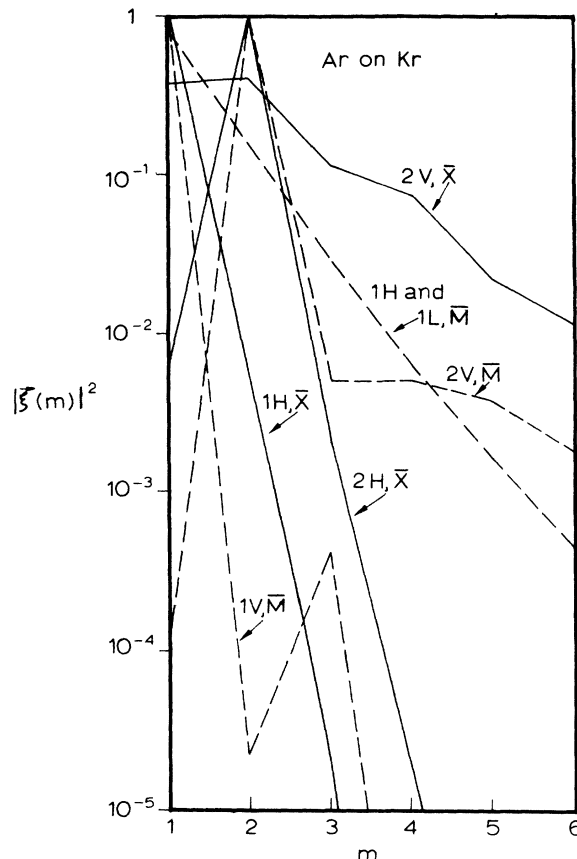The main surface modes are the three "principal" modes associated with the adsorbate, and

an S_1 surface mode for the clean-substrate material which persists (with its frequency changed) when the adsorbate is deposited.

The relative positions of the $1L, 1H$ modes and the $1V$ mode at $\bar{M}$ (in Figs. 1–7) are inverted in the results for the "mass-defect" model,[2] as discussed in Sec. III B. Also, in the present results for weakly interacting adsorbates (He and Ne), the substrate modes are much less affected by deposition of the adsorbate than in the results for the mass defect model. Both these facts show that the mass defect model can lead to qualitatively inaccurate conclusions about the vibrational modes of adsorbed atoms.

---

*Present address: School of Science and Technology, University of Houston at Clear Lake City, Clear Lake City, Tex.

[1]W. R. Lawrence and R. E. Allen, Phys. Rev. B (to be published).

[2]G. P. Alldredge, R. E. Allen, and F. W. de Wette, Phys. Rev. B 4, 1682 (1971). See also, L. Dobrzynski, Surf.

Sci. 20, 99 (1970); and L. Dobrzynski and D. L. Mills, J. Phys. Chem. Solids 30, 1043 (1969). However, G. Armand and J. B. Theeten [Phys. Rev. B 9, 3969 (1974)] included force-constant changes.

[3]R. E. Allen, G. P. Alldredge, and F. W. de Wette, Phys. Rev. B 4, 1661 (1971).